This document presents a review of available literature related to the 1970 Calingiri surface rupturing earthquake. It includes newly digitised data related to the rupture and new interpretations of controls on fault rupture. It is intended to supplement a manuscript reviewing all Australian surface rupturing earthquakes, submitted to Geosciences in August 2019. It will likely be repackaged for submission to a peer-reviewed journal at a later date and we consider it to be a draft pre-print.

Please contact any of the authors on the content presented herein; we welcome constructive feedback.

Review paper: The 10th March 1970 M_w 5.0 Calingiri surface rupturing earthquake, Australia

Tamarah King

School of Earth Sciences, The University of Melbourne, Victoria 3010, Australia
tamarah.king@unimelb.edu.au
https://orcid.org/0000-0002-9654-2917

Mark Quigley

School of Earth Sciences, The University of Melbourne, Victoria 3010, Australia
Mark.quigley@unimelb.edu.au
https://orcid.org/0000-0002-4430-4212

Dan Clark

Geoscience Australia, Canberra 2601, Australia
Dan.Clark@ga.gov.au
https://orcid.org/0000-0001-5387-4404

Abstract

The 10th March 1970 moment magnitude (M_W) 5.0 Calingiri earthquake surface rupture is 3.3 km long with a maximum vertical displacement of 0.4 m. The fault as defined by surface measurements is a shallow-dipping reverse fault (~ 20° east) with a probable shallow hypocentre (< 1 km). This is consistent with published hypocentral depths, though large uncertainties exist within the seismological data. The finest-resolution geological map available for the epicentral area (1:250 000) indicates the presence of granitic gneiss and migmatite outcrops within a few kilometres of the surface rupture with foliations striking sub-parallel to the surface rupture trace but with near-vertical dips. The rupture is subparallel to linear geophysical anomalies suggesting a bedrock structural control to faulting. There is no evidence to suggest prior Pleistocene surface rupture along the Calingiri scarp, although no detailed palaeoseismic investigations have been conducted.

1. Geology

1.1 Regional

The 1970 Mw 5.0 Calingiri earthquake is one of a series of historical surface rupturing earthquakes (1968 Meckering, 1970 Calingiri, 1979 Cadoux, 2008 Katanning, and 2018 Lake Muir) (Dawson et al., 2008; Gordon and Lewis, 1980; Lewis et al., 1981) hosted within the South-West Seismic Zone (SWSZ) in southern Western Australia (Doyle, 1971). The SWSZ resides predominately within the Yilgarn Craton (*Figure 1*), an assemblage of predominately Archean granitoid-greenstone rocks (Wilde et al., 1996). The SWSZ extends roughly NW-SE within a region of the Yilgarn Craton consisting of poly-deformed and metamorphosed crystalline basement (*Figure 1*). The SWSZ extends across three tectono-stratigraphic terranes; the Boddington Terrane, Lake Grace Terrane and Murchison Terrane (Dentith and Featherstone, 2003; Wilde et al., 1996). Due in part to few basement outcrops, the boundaries between terranes are poorly constrained. Gravity data show that the boundary between the Boddington and Lake Grace Terranes is a major east-dipping geological structure (Clark et al., 2008; Dentith and Featherstone, 2003), interpreted as a large thrust zone based on dating and metamorphic facies analysis across the two terranes (Wilde et al., 1996). Historic

seismicity generally aligns with this structure, and occurs on the eastern side of it (Dentith and Featherstone, 2003).

The Calingiri earthquake occurred in the northern area of the Jimperding Metamorphic Belt (*Figure 1*), within the Lake Grace Terrane, but close to the mapped boundaries with the Boddington and Murchison Terranes. The Jimperding belt consists of "repeatedly deformed granitoids, gneisses, belts of metasedimentary rocks, small greenstone belts and remnants of layered basic intrusions" (Dentith and Featherstone, 2003).

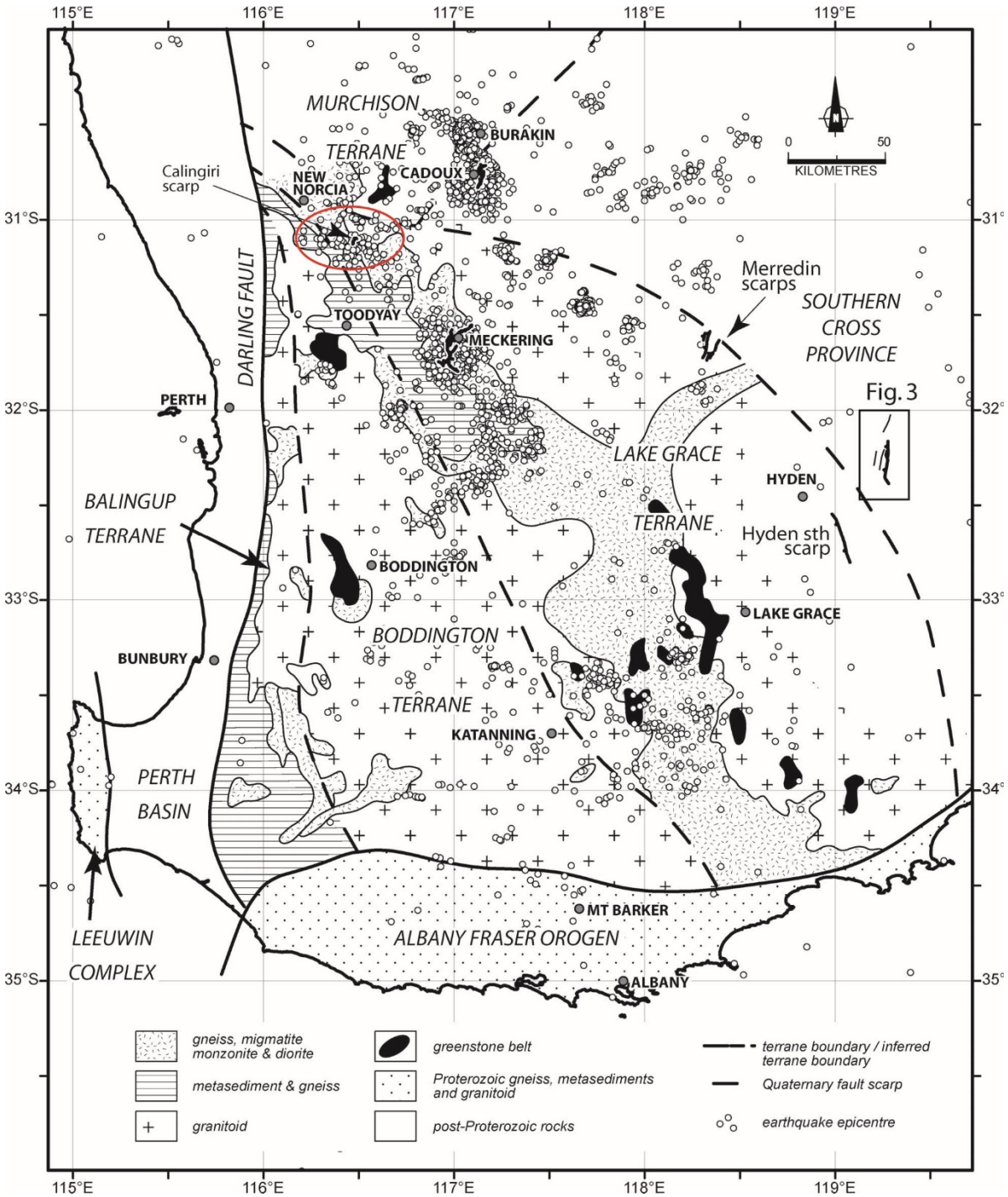

Figure 1: Regional geology surrounding the Calingiri earthquake and SWSZ. Figure2 from Clark et al. (2008)

1.2 Local bedrock

No bedrock outcrops were mapped near the Calingiri scarp by Gordon and Lewis (1980). They do describe "vertically foliated Archean migmatites and metasediments" to the west of Calingiri, "equigranular granite" to the north-east of the town, and "a few" dolerite dykes and quartz veins. The Western Australia Geological Survey 1:250,000 geological map (Wilde et al., 1978) (*Figure 3*) shows basement outcrops of banded migmatite and granitic gneiss in the rupture area with the majority of foliation trending towards the NE, coincident with strike of rupture. The dips of planar fabric elements within these surface outcrops are near-vertical in most locations, whereas dips of the faults underlying the rupture are ~ 20° (Section 3.2.3.). The surface rupture strikes subparallel to a magnetic anomaly, and the edge of a minor gravitational anomaly *Figure 2*.

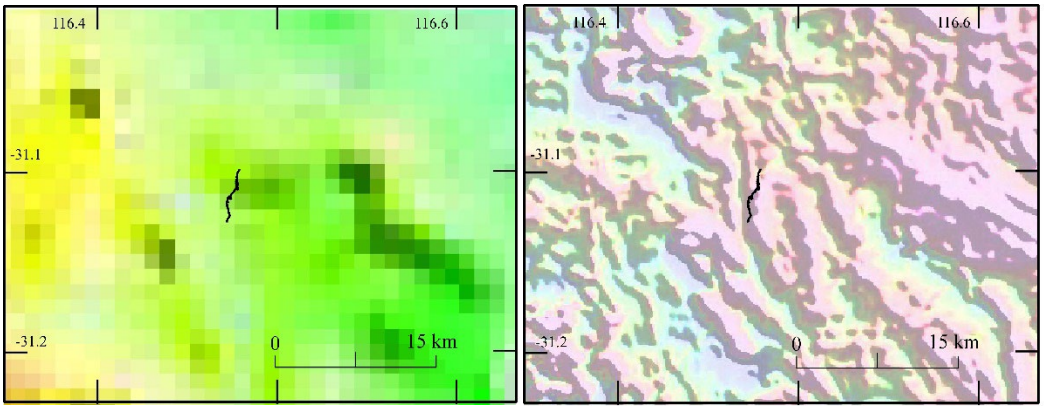

Figure 2: Calingiri scarp (black lines) relative to magnetic intensity and bouguer gravity anomaly maps. National bouguer gravity anomaly map: http://pid.geoscience.gov.au/dataset/ga/101104; National total magnetic intensity map: http://pid.geoscience.gov.au/dataset/ga/89596

1.3 Surficial deposits

Authors investigating the event do not describe the local geology or surface sediments in detail. The available 1:250,000 geological map of the area (Wilde et al., 1978) shows the rupture associated with "Cenozoic laterite" and "quartzose duricrust" (*Figure 3*).

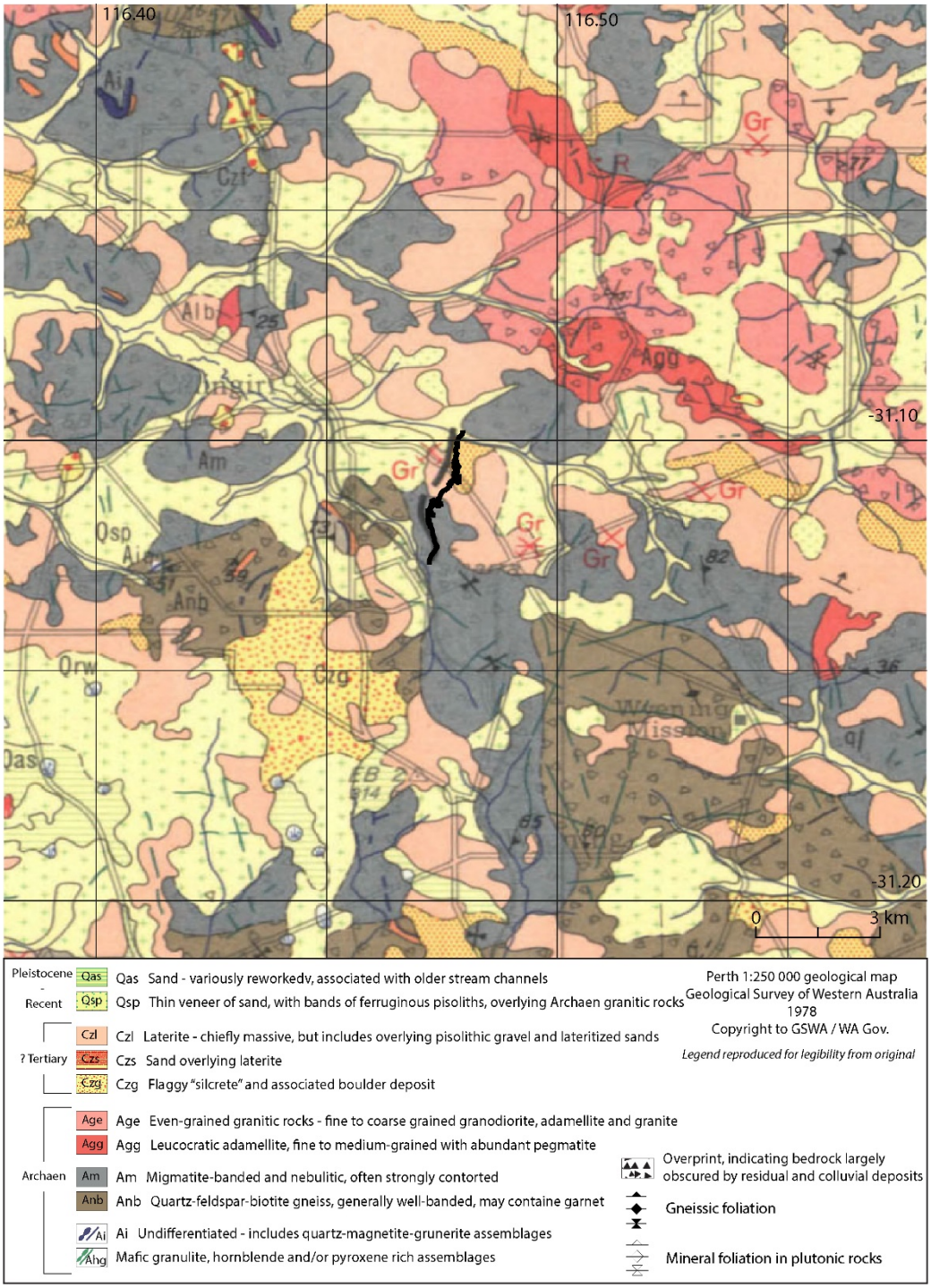

Figure 3: Crop of Perth 1:250 000 geological map sheet (Wilde et al., 1978) showing basement and surface sediments around the Calingiri surface rupture. Full map and legend available from: http://www.dmp.wa.gov.au/Geological-Survey/GSWA-publications-and-maps-1399.aspx

2. Seismology

2.1 Epicentre and magnitude estimates

No relocation of the epicentre has taken place, with the current Geoscience Australia (GA) online catalogue location the same coordinates as the original reported location (Gregson, 1971) (Table 1). The location is on the footwall 700 m from the surface rupture though uncertainty may be in the order of ± 1 – 10 km, so the true epicentre is likely on the hanging-wall of the surface rupture (*Figure 4*). The GA NSHA18 catalogue (Allen et al., 2018) epicentre is located ~5 km NE of the other epicentres,

it is not known how this was derived (*Figure 4*). No uncertainties are published regarding the Calingiri epicentre location in the original reports on the event.

This paper prefers the magnitude (M_W) of the recently published NSHA18 catalogue (Allen et al., 2018) as they conduct a thorough and consistent reanalysis of Australian magnitude values, particularly to address inconsistencies in the determination of historic magnitude values. Prior to this reanalysis, the magnitude of the Calingiri earthquake was reported as 5.7 – 6.2 using various local magnitude formula (M_L). These almost one magnitude unit higher than the revised NSHA18 magnitude, which has implications for any previous scaling relationships incorporating older magnitudes.

Table 1 : Published epicentre locations, depths and magnitudes

Reference	Agency	Latitude	± (km)	Longitude	± (km)	Depth	± (km)	M1		M2		M3	
GA_online	GA	-31.11		116.47		1		5.7	Mw	5.9	ML	5.5	mb
Everingham and Parkes (1971)	Mundaring Observatory	-31.11		116.47		1		5.7	M	6.2	M	5.1	MS
Gordon and Lewis (1980)	Mundaring Observatory	-31.11		116.47		1		6.2	ML	5.7	M		
Allen et al (2018)	NSHA18	-31.092		116.512		15		5.03	Mw	5.9	ML		

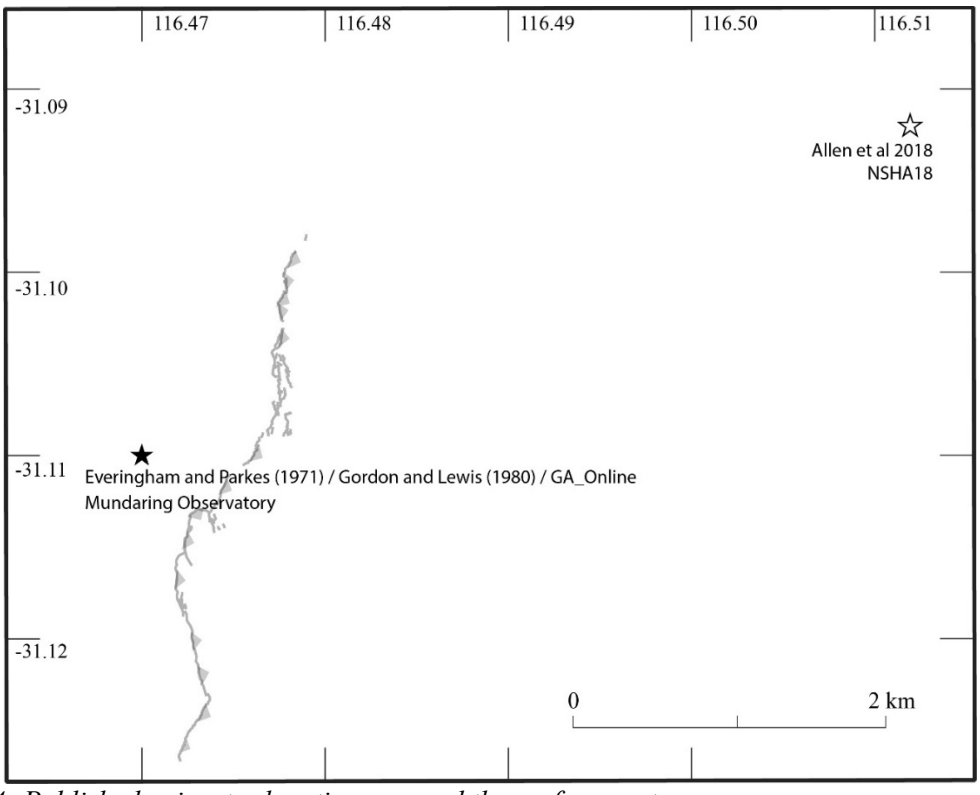

Figure 4: Published epicentre locations around the surface rupture

2.2 Focal mechanisms

Fitch et al. (1973) published the only focal mechanism for the Calingiri rupture, a lower hemisphere solution which shows a reverse mechanism with a dextral component to movement along a preferred plane trending 056° and dipping 50° to the east (based on surface rupture) (*Figure 5*). Gordon and

Lewis (1980) report sinistral movement on a fault striking 337° and dipping 76°E based on the Fitch et al. (1973) solution, however this plane of the focal mechanism actually describes a sinistral west dipping fault. As noted by Leonard et al. (2002), the Fitch et al. (1973) solution is based on short period instrument recordings, has uncertainties of 120 – 100° and was constrained by their solution for the Meckering earthquake.

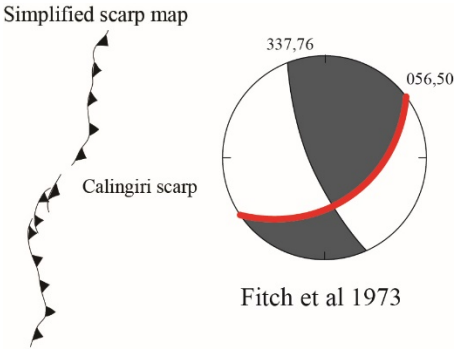

Figure 5: Published focal mechanism, preferred rupture plane from the publication highlighted in red.

2.3 Depth

Gregson (1971) report a depth of 1 km derived by the USGS, also the depth used in Everingham and Parkes (1971) and Gordon and Lewis (1980). Fitch et al. (1973) report a depth of 15 km in their focal mechanism solution, too deep to have produced a surface rupture.

2.1 Foreshock / aftershocks

The Calingiri area experienced three (assumed to be M_L) > 4.0 earthquakes prior to the 1968 Meckering earthquake, which triggered increased seismicity in the region. In 1952 an earthquake (of unspecified magnitude) is reported to have caused structural damage to a new school building, with an epicentral location determined 13 km north of the township (Gordon and Lewis, 1980). In 1955 the Mundaring Observatory reported a magnitude 4.7 earthquake approximately 19 km north of the town, while in 1963 a magnitude 4.9 event was located 13 km north (Gordon and Lewis, 1980). Calingiri experienced seventeen events between M_L 2.6 - 4.4 from October 1968 (the Meckering earthquake) to November 1969 (the Calingiri mainshock occurred 4 months later) (Everingham and Gregson, 1971; Gordon and Lewis, 1980; Gregson, 1971).

One temporary seismometer was deployed by Mundaring Observatory, but the instrument failed and recorded no earthquakes (Gregson, 1971). Following the Calingiri mainshock only nine aftershocks are recorded in the area, with magnitudes ranging from M_L 3.0 - 4.0. The Mundaring Observatory reports foreshocks down to magnitude M_L 2.6, so we consider this to represent the catalogue completeness value for this area at this time. Therefore, the Calingiri event shows a lack of immediate aftershock activity, with a M_L 3.8 recorded in July (4 months after the mainshock), 3.1 in October (7 months) and the largest aftershock with M_L 4.0 occurring in December 1970 (9 months). No events > M_L 2.6 were recorded in the area from 1973 - 1980. Given this aftershock temporal distribution, Gordon and Lewis (1980) consider the Calingiri mainshock as an aftershock to the larger Meckering event, though this is not consistent with current methods for determining maximum distances of aftershocks (e.g. those used in Allen et al. (2018)).

3. Surface Rupture

3.1 Authors / map quality

The Calingiri rupture is located on a pastoral property 152 km drive north of Perth. The first descriptions of the Calingiri surface rupture come from seismological reports from the Mundaring Geophysical observatory, located 120 km south of the rupture (Everingham and Gregson, 1971;

Gregson, 1971). The only published detailed mapping of the rupture is a 1:10,000 map in Gordon and Lewis (1980) with mapping conducted 1 - 2 months after the rupture. The rupture trace from this map is reproduced in the GA Neotectonics Features database (Clark, 2012). Gordon and Lewis (1980) note that farming had removed surficial evidence of rupture, though some sections of are still visible in Google and Bing satellite imagery. The rupture trace from the GA Neotectonics Features and sections visible in Google and Bing satellite imagery do not align (e.g. -31.12, 116.47) due to datum transformation issues and simplification of fine-scale morphology in the original map.

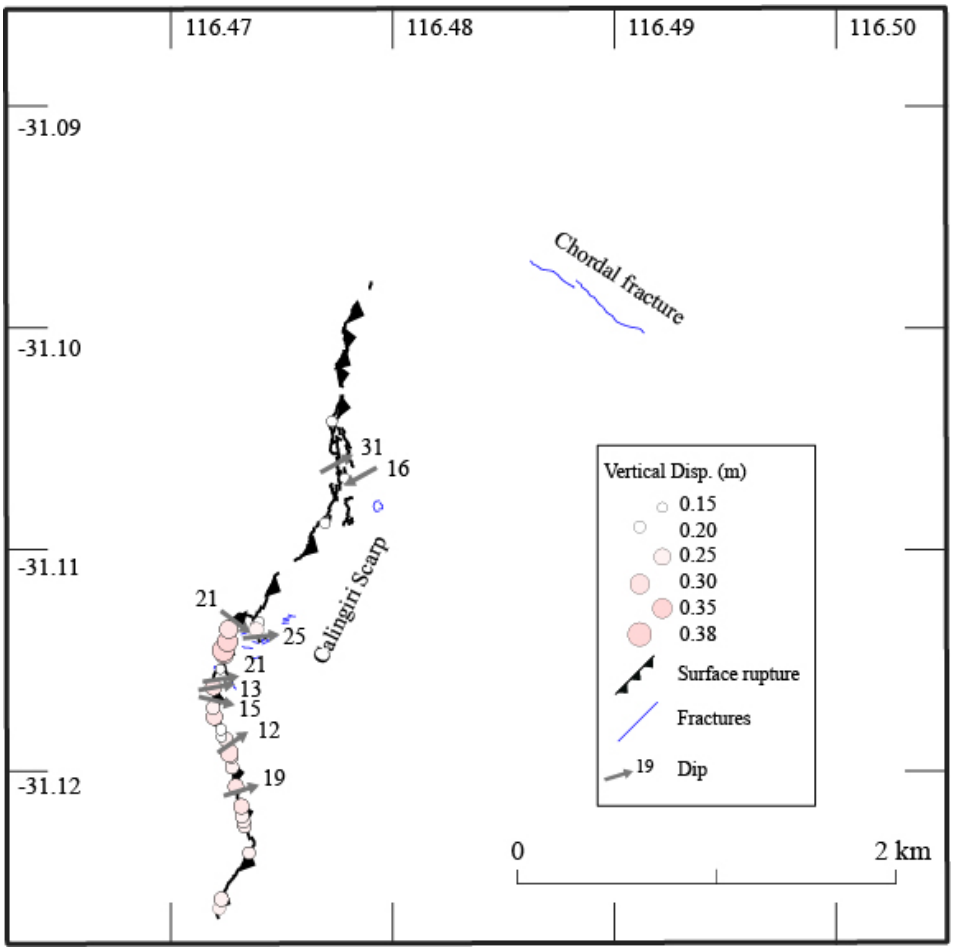

Figure 6: *Map of the Calingiri scarp, fractures, vertical offset measurements, and dip measurements (data digitised from* Gordon and Lewis (1980))

3.2 Rupture Morphology

3.2.1. Length and shape

Initial reports describe a 5 km long rupture (Everingham and Gregson, 1971; Gregson, 1971), however Gordon and Lewis (1980) describe 3.3 km long scarp, and this is the length reported in subsequent publications (Figure 7b). This length results from measuring the rupture from north to south along a straight line. Applying a criteria which simplifies ruptures to straight lines and defines new faults where mapped primary rupture has gaps/steps > 1 km and/or where strike changes by > 20° for distances > 1 km (e.g. (Quigley et al., 2017)) results in the same length (explored in more detail in King et al. (2019) (in review)). The length of the causative fault, assuming a relatively straight plane, is likely to be slightly longer than the simplified 3.3 km long trace, as the fault will not have ruptured to the surface along its full length.

Figure 7c maps portions of the scarp where more than two vertical displacement measurements of greater than 0.2 m occur within a distance of 1 km (data from Gordon and Lewis (1980)). Given granitic basement cosmogenic erosion rates in equivalent arid settings of Australia of 0.3 – 5 m/Myr

(Bierman and Caffee, 2002), 0.2 m of scarp height would be removed within 35 – 660 kyrs, leaving ~1 km of rupture still visible in the landscape. This indicates that the feature is unlikely to be persistent in the landscape over the time frame typical of the recurrence interval observed on nearby faults in the SWSZ (e.g. Hyden, Dumbleyung (Clark et al., 2008; Estrada et al., 2006)). In this calculation we do not account for erosion rates of any duricrust which may overlie granitic bedrock, for differential erosion rates across the rupture topography, or increased erosion from past climatic changes or modern processes.

The mapped surface rupture trace by Gordon and Lewis (1980) shows discontinuous segments of 50 – 500 m in length with breaks up to 150 m (*Figure 6*, *Figure 7*). It has an overall shape that is slightly concave, with concavity defined by short (< 500m) oblique linear segments. Longer Australia surface ruptures (e.g. Meckering, Cadoux) have similar deviations of strike orientation across short distances (e.g. < 500 m).

A 600 m long secondary scarp (the 'Calingiri Chordal Fault') is mapped on the hanging-wall ~1 km away from the northern tip of the main rupture (*Figure 6*, Figure 7). Gordon and Lewis (1980) report that the property owner observed this scarp six weeks following the main rupture and stated that it had not been visible on multiple previous visits to the field. This scarp is mapped as a series of en echelon extensional fractures and may better be described as secondary extensional fractures related to hanging-wall relaxation rather than a primary rupture, although its possible genesis from an aftershock cannot be dismissed.

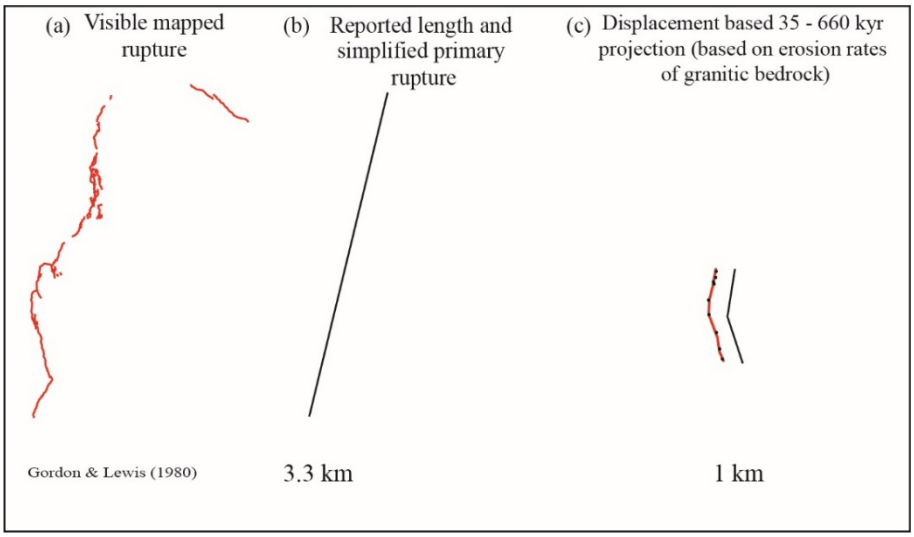

Figure 7: Various measures of length for the Calingiri rupture and underlying fault as described in the text.

3.2.2. Strike

The rupture trends towards 011° on average, with deviations along its length describing trends between 346 – 030°. The secondary extensional fracture ('chordal fault') trends toward 306°.

3.2.3. Dip

Gordon and Lewis (1980) show dip measurements along the rupture ranging from 12 - 31° on their map of the rupture (Figure 6), with an average of 19°. The report mentions shallower dips of 10° measured where the rupture crosses a stream and drain. They relate dip variations to surficial sediment competency. They calculate an overall dip of 40° east based on slip (horizontal and vertical components of displacement).

The only reported seismologically derived dip comes from Fitch et al. (1973) who find a 50° dip on the east dipping plane (*Figure 5*). As previously described, Gordon and Lewis (1980) identify the incorrect plane of the Fitch et al. (1973) solution and describe the dip as 76° NE, which matches the

SW dipping plane. The Fitch et al. (1973) solution for dip has uncertainties as described for the focal mechanism.

3.2.4. Morphology

The southern section of the Calingiri scarp generally shows a single discrete rupture with short step-overs or ramp structures (Gordon and Lewis, 1980). The northern section is characterized by single discrete ruptures or pressure ridges, often discontinuous over short distances, or with multiple duplexing discrete ruptures. As with the Meckering scarp, Gordon and Lewis (1980) note that the rupture morphology seemed related to surficial sediments, low compression ridges in sandy soil and larger discrete ruptures in lateritic soils.

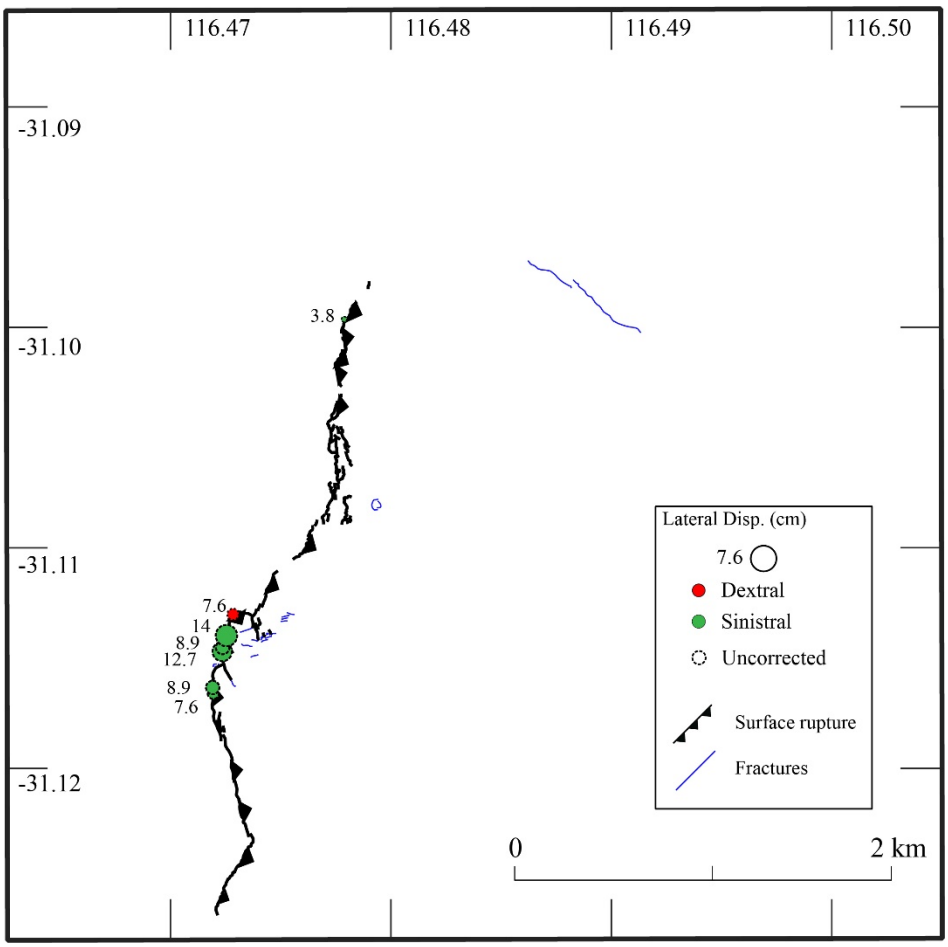

Figure 8: Lateral displacement measurements (in cm) digitised from Gordon and Lewis (1980). Uncorrected measurements (all measurements) are offsets measured from features (fences, roads, etc) not perpendicular to the strike of surface rupture.

3.3 Kinematics

Gordon and Lewis (1980) describe the Calingiri fault as a sinistral thrust, recording predominately sinistral movement where measurements were taken of offset features (Figure 8). All measurements are uncorrected for the horizontal angle between the rupture and offset feature, so true lateral offset is unknown (e.g. if not perpendicular, lateral offset may appear greater or less than true offset). Stepovers and fractures in the central and southern sections of rupture support a sinistral compressional step, though the breaks between segments in the northern section show a dextral extensional sense of movement, and step overs in the northern segment could be either dextral compression or sinistral extension.

3.4 Displacement

Vertical and lateral offset along the rupture is mapped in plate 6 of Gordon and Lewis (1980), but no description exists for how these measurements were obtained, so we cannot estimate measurement uncertainty. No levelling profiles were published for this rupture, and no surveying along the scarp is described in published sources. The digitised data (methods in Appendix A) show an asymmetrical along-rupture displacement envelope concentrated on the southern scarp, with maximum offset in the central most arcuate section of rupture (Figure 9). Only three offset measurements are recorded along the northern section of scarp, though the text describes offsets of 7 – 8 cm along the majority of the scarp.

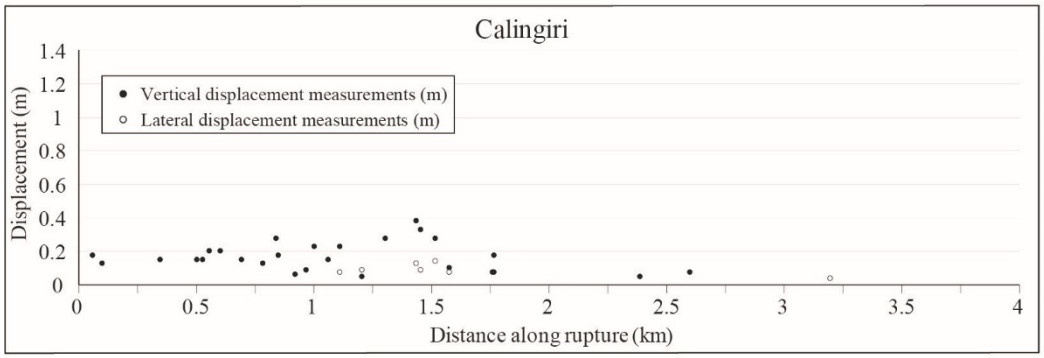

Figure 9: Vertical and lateral displacement measurements along the Calingiri scarps, digitised from (Gordon and Lewis, 1980). Methods described in Appendix A

3.5 Relationship to Geology

The Western Australian Geological Survey 1:250,000 map (Wilde et al., 1978) shows migmatite and gneissic basement in the rupture area, with foliation measurements varying between 140°/90°, 060°/90°, 180°/73° and 030°/59°. While variable, these measurements show some similarity to surface rupture segments striking between 340 – 030°. The total magnetic intensity map shows a potentially folded structure striking NW at the rupture location (Figure 2), consistent with strongly deformed metasediments within the Jimperding Metamorphic Belt, including along the 1968 Meckering rupture (Dentith et al., 2009). The rupture generally strikes in the same direction as the western limb of this structure.

3.1 Relationship to Seismology

The only focal mechanism for the Calingiri earthquake (Fitch et al., 1973) shows a dextral component of slip on the east dipping plane with a strike of 056° which is oriented 20 - 40° clockwise relative to the trend of the surface rupture. Gordon and Lewis (1980) misinterpret the focal mechanism suggesting sinistral movement on a fault striking 337°. The surface rupture step-overs and gaps show both dextral and sinistral senses of movement. Gordon and Lewis (1980) present predominately sinistral measurements, with some dextral offset also recorded (Figure 8, Figure 9). Uncertainties exist on the accuracy of the focal mechanism (see Section 2.2), and lateral offset measurements are uncorrected and therefore may be inaccurate.

A cross section using measured dips from Gordon and Lewis (1980) shows how published epicentres relate to the rupture at depth (Figure 10). The NSHA18 epicentre projects to approximately 1 km depth based on simplified fault geometry. The uncertainty bounds on the footwall epicentre may be up to 10km which could place it on the hanging-wall fault plane with potential depths 0 – 3.5 km (on a 20° dipping fault). Using the 40° preferred dip from Gordon and Lewis (1980) gives a depth range of 0 – 8 km. This is in line with other historic surface rupturing earthquakes where seismological modelling shows centroid and hypocentral depths < 6 km (Fredrich et al., 1988; McCaffrey, 1989; Vogfjord and Langston, 1987).

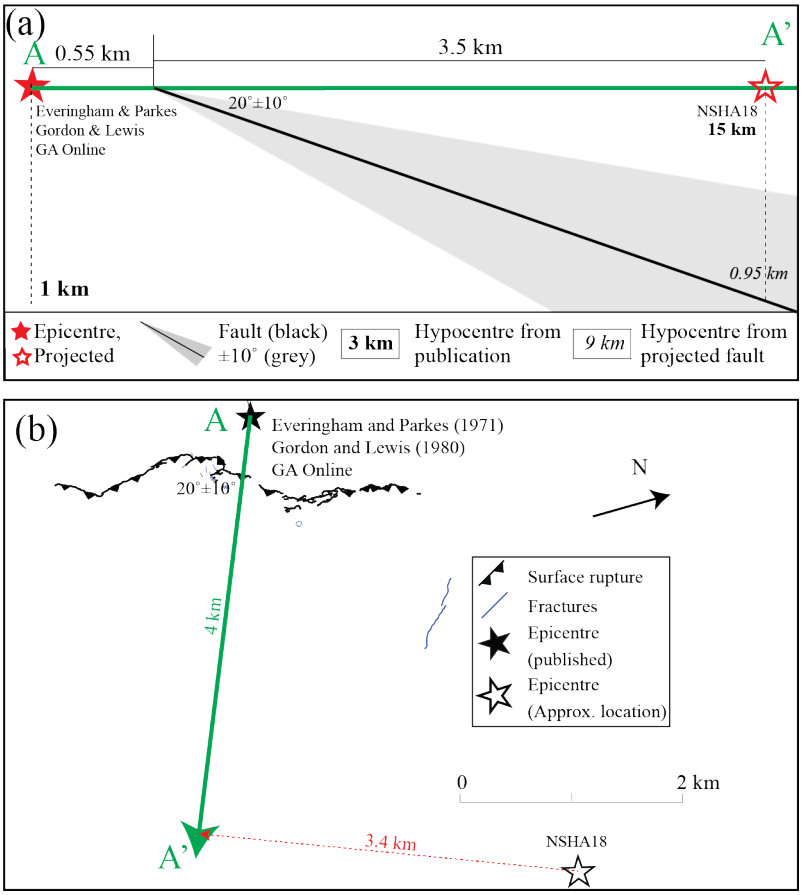

Figure 10:Cross section across the Calingiri rupture showing epicentre locations as projected onto the cross section, depth of epicentres as published (bold) and depth to projected fault plane (italics) from surface dip data (from Gordon and Lewis (1980))

3.2 Environmental damage

Based on length and maximum offset, the Calingiri surface rupture fits an ESI-07 scale measure of IX, while fractures/cracking as described by Gordon and Lewis (1980) fits ESI V-VI (Michetti et al., 2007). No other environmental damage is specifically documented that falls within the ESI-07 scale. Gordon and Lewis (1980) note a single location where circular extensional cracking surrounded a small tree, similar to descriptions of the Meckering rupture (Gordon and Lewis, 1980) and Petermann rupture (King et al., 2018). Gordon and Lewis (1980) describe cracking identified near the Calingiri rupture that appeared infilled and many years old, they suggest this may relate to the 1968 Meckering earthquake based on the observed infill and level of degradation.

4. Paleoseismology

4.1 Authors / mapping quality

No palaeoseismic investigations of the Calingiri rupture have been published. Gordon and Lewis (1980) report scattered quartz fragments and thicker soil horizons in holes dug on the footwall compared to several “missing” soil horizons on the hanging-wall, which they interpreted as supportive evidence for past movement along a pre-existing fault. This evidence is circumstantial and could be explained by several processes including differential weathering across lithological contacts or faults, or a soil catena along the low relief hillslope which is coincident with the historic rupture.

4.2 Slip rate

There is no evidence geological or geomorphic evidence to support prior rupture along the Calingiri fault. The rupture is either the first neotectonic event, or the recurrence interval is sufficiently long that all relief relating to prior event(s) was eroded prior to 1979 (e.g. 35 – 660 kyrs as discussed in Section 3.2.1). If recurrence is assumed, vertical relief generation rates are limited by very low bedrock erosion rates of < 5 m/Myr (Belton et al., 2004; Bierman and Caffee, 2002).

5. References

Allen, T., Leonard, M., Ghasemi, H., Gibson, G., 2018. The 2018 National Seismic Hazard Assesment: Earthquake epicentre catalogue (GA Record 2018/30). Geoscience Australia, Commonwealth of Australia, Canberra, ACT. https://doi.org/http://dx.doi.org/10.11636/Record.2018.030

Belton, D.X., Brown, R.W., Kohn, B.P., Fink, D., Farley, K.A., 2004. Quantitative resolution of the debate over antiquity of the central Australian landscape: Implications for the tectonic and geomorphic stability of cratonic interiors. Earth Planet. Sci. Lett. 219, 21–34. https://doi.org/10.1016/S0012-821X(03)00705-2

Bierman, P.R., Caffee, M.W., 2002. Cosmogenic exposure and erosion history of Australian bedrock landforms. Bull. Geol. Soc. Am. 114, 787–803. https://doi.org/10.1130/0016-7606(2002)114<0787:CEAEHO>2.0.CO;2

Clark, D., 2012. Neotectonic Features Database. Geoscience Australia, Commonwealth of Australia, Canberra, Australia.

Clark, D., Dentith, M., Wyrwoll, K.-H., Yanchou, L., Dent, V.F., Featherstone, W.E., 2008. The Hyden fault scarp, Western Australia: paleoseismic evidence for repeated Quaternary displacement in an intracratonic setting. Aust. J. Earth Sci. 55, 379–395. https://doi.org/10.1080/08120090701769498

Dawson, J., Cummins, P.R., Tregoning, P., Leonard, M., 2008. Shallow intraplate earthquakes in Western Australia observed by Interferometric Synthetic Aperture Radar. J. Geophys. Res. Solid Earth 113, 1–19. https://doi.org/10.1029/2008JB005807

Dentith, M., Clark, D., Featherstone, W.E., 2009. Aeromagnetic mapping of Precambrian geological structures that controlled the 1968 Meckering earthquake (Ms 6.8): Implications for intraplate seismicity in Western Australia. Tectonophysics 475, 544–553. https://doi.org/10.1016/j.tecto.2009.07.001

Dentith, M., Featherstone, W.E., 2003. Controls on intra-plate seismicity in southwestern Australia. Tectonophysics 376, 167–184. https://doi.org/10.1016/j.tecto.2003.10.002

Doyle, H.A., 1971. Seismicity and structure in Australia. Bull. R. Soc. New Zeal. 9.

Estrada, B., Clark, D., Wyrwoll, K.-H., Dentith, M., 2006. Paleoseismic investigation of a recently identified Quaternary fault in Western Australia: the Dumbleyung Fault. Proc. Aust. Earthq. Eng. Soc. Canberra ACT, Novemb. 2006 189–194.

Everingham, I.B., Gregson, P.J., 1971. Mundaring Geophysical Observatory, Annual Report, 1968 (BMR Record 1971/12). Bureau of Mineral Resources, Geology and Geophysics, Canberra, Australia. https://doi.org/http://pid.geoscience.gov.au/dataset/ga/12549

Everingham, I.B., Parkes, A., 1971. Intensity Data for Earthquakes at Landor (17 June 1969) and Calingiri (10 March 1970) and their Relationship to Previous Western Australian Observations (BMR Recrod 1971/80), 1971/80. ed. Bureau of Mineral Resources, Geology and Geophysics, Canberra, Australia. https://doi.org/http://pid.geoscience.gov.au/dataset/ga/12617

Fitch, T.J., Worthington, M.H., Everingham, I.B., 1973. Mechanisms of Australian earthquakes and contemporary stress in the Indian ocean plate. Earth Planet. Sci. Lett. 18, 345–356.

https://doi.org/10.1016/0012-821X(73)90075-7

Fredrich, J., Mccaffrey, R., Denham, D., 1988. Source parameters of seven large Australian earthquakes determined by body waveform inversion. Geophys. J. 95, 1–13. https://doi.org/https://doi.org/10.1111/j.1365-246X.1988.tb00446.x

Gordon, F.R., Lewis, J.D., 1980. The Meckering and Calingiri earthquakes October 1968 and March 1970, Geological Survey of Western Australia Bulletin. Perth.

Gregson, P.J., 1971. Mundaring Geophysical Observatory Annual Report, 1970 (BMR Record 1971/77). Bureau of Mineral Resources, Geology and Geophysics, Canberra, Australia. https://doi.org/http://pid.geoscience.gov.au/dataset/ga/12614

King, T.R., Quigley, M.C., Clark, D., 2019. Surface-rupturing historical earthquakes in Australia and their environmental effects: new insights from re-analyses of observational data. Geosciences.

King, T.R., Quigley, M.C., Clark, D., 2018. Earthquake environmental effects produced by the Mw 6.1, 20th May 2016 Petermann earthquake, Australia. Tectonophysics 747–748, 357–372. https://doi.org/10.1016/j.tecto.2018.10.010

Leonard, M., Ripper, I.D., Yue, L., 2002. Australian earthquake fault plane solutions (GA Record 2002/019), 2002/19. ed. Canberra, ACT. https://doi.org/http://pid.geoscience.gov.au/dataset/ga/37302

Lewis, J.D., Daetwyler, N.A., Bunting, J.A., Montcrieff, J.S., 1981. The Cadoux Earthqauke (GSWA Report 11). Perth, Australia.

McCaffrey, R., 1989. Teleseismic investigation of the January 22, 1988 Tennant Creek, Australia, earthquakes. Geophys. Res. Lett. 16, 413–416. https://doi.org/10.1029/GL016i005p00413

Michetti, A.M., Esposito, E., Guerrieri, L., Porfido, S., Serva, L., Tatevossian, R.E., Vittori, E., Audemard M., F.A., Azuma, T., Clague, J., Comerci, V., Gurpinar, A., McCalpin, J.P., Mohammadioun, B., Morner, N.A., Ota, Y., Roghozhin, E., 2007. Intensity Scale ESI 2007, Memorie Descrittive della Carta Geologica d'Italia, Special Volume 74. APAT, Rome 2007.

Quigley, M.C., Mohammadi, H., Duffy, B.G., 2017. Multi-fault earthquakes with kinematic and geometric rupture complexity : how common ? INQUA Focus Group Earthquake Geology and Seismic Hazards.

Vogfjord, K.S., Langston, C.A., 1987. The Meckering earthquake of 14 October 1968: A possible downward propagating rupture. Bull. Seismol. Soc. Am. 77, 1558–1578.

Wilde, S.A., Low, G.H., Lake, R.W., 1978. Perth 1:250 000 Geological Map Sheet. Geological Survey of Western Australia, Perth, Western Australia.

Wilde, S.A., Middleton, M.F., Evans, B.J., 1996. Terrane accretion in the southwestern Yilgarn Craton: evidence from a deep seismic crustal profile. Precambrian Res. 78, 179–196. https://doi.org/10.1016/0301-9268(95)00077-1

Appendix A

Methods for digitising vertical displacement data

The only offset measurements published for the Calingiri scarp are mapped along the scarp in Plate 6 of Gordon and Lewis (1980). This map was georeferenced against satellite imagery based on the locations of roads, fences, and train tracks. The locations and vertical offset were recorded into a new point shapefile. A simplified rupture trace was created for the scarps, and a short script[1] was used in

[1] line_locate_point(geometry:=geometry(get_feature('Line', 'id', '1')), point:=$geometry)

QGIS attribute manager field calculator to extract the distance of each vertical offset measurement along the simplified rupture trace. The shape file was extracted into a final CSV with x-y coordinates, vertical offset measurements, and distance along rupture data.

Dip data were digitised into a point shape file from a georeferenced version of Plate 5 from Gordon and Lewis (1980).